Scanning Tunneling Microscopy and Spectroscopy

Table of Contents

1. Motivation

With the development of quantum mechanics in the early 20th century, mankind's perception of nature was stretched to a great degree leading to new axioms, and the recognition of the particle-wave dualism. It was found that particles with small masses such electrons could interchangeably be described as waves or as corpuscular objects. With the wave character of matter, particles exhibit a probability of existence at places, where they can classically not exist. One of these phenomena is the tunnel effect, which describes the ability of an electron to tunnel through a vacuum barrier from one electrode to the other. Since 1960 tunneling has been extensively studied experimentally. This led in 1981 to the first microscopic tool with which atoms could be observed in real space – the scanning tunneling microscopy. In addition to the atomic resolution imaging capability of STM, tunnel currents could be studied with this tool in a spectroscopy manner providing insight into the local density of state (LDOS) of material surfaces.

2. Scanning Tunneling Microscopy

While vacuum tunneling was theoretically predicted by Folwer and Nordheim 1928,[1], it was not until 1981 with G Binnig and H. Rohrer's introduction of the scanning tunneling microscope (STM) that provided the first observation of vacuum tunneling between a sharp tip and a platinum surface.

Wavefunction Overlap, Electron Probability

STM is based on a quantum mechanical phenomenon, called tunneling. In quantum mechanics, small particles like electrons exhibit *wave-like* properties, allowing them to "penetrate" potential barriers, a quantum mechanical probability process that is based on classical Newtonian mechanics impossible.* In general, STM involves a very sharp conductive tip that is brought within tunneling distance (sub-nanometer) of a conductive sample surface, thereby creating a metal-insulator-metal (MIM) configuration. In the representation of one-dimensional tunneling (Figure 1), the tunneling wave of the sample electrons, ψ_s, and the wave of a STM tip electrons, ψ_t, overlap in the insulating gap, allowing a current to flow.

To achieve some understanding of the physical meaning of the wave function ψ, we consider the square magnitude of it, which represents the probability of finding an electron at a given location. Generally, this is visualized with electron clouds for atoms or

* A more detailed discussion on barrier tunneling is provided in a later section of this text.

molecules, or for condensed phases with energy levels, as illustrated with the gray shaded areas in Figure 2. In metals, electrons fill the continuous energy levels up to the Fermi level, E_F, which defines an upper boundary, similar to the sea level. Above E_F we find electrons that are activated (e.g., thermally). We can raise the Fermi level (e.g., of the sample) in regards to a second material (e.g., tip) by applying a voltage.

Thus, to observe the tunneling current I of electrons through the vacuum gap between the sample and the tip, a bias voltage, $V_{bias,}$ is applied, as shown in Figure 2. At $V_{bias} = 0$, the electrons cannot flow in either direction since the Fermi level, $E_{f,}$ of both the tip and the sample is equal, i.e., the gradient is zero. When $V_{bias} > 0$ (positive bias), the Fermi level of the sample is raised by V_{bias}, and the electrons in the occupied state (filled with electrons) of the sample can tunnel into the unoccupied state of the tip. Similarly, when $V_{bias} < 0$ (negative bias), the electrons in the occupied state of the tip tunnel into the unoccupied state of the sample.

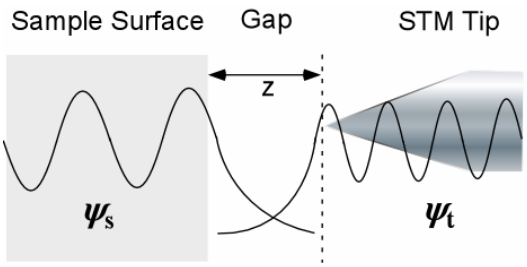

Figure 1: Schematic of STM one-dimensional tunneling configuration.

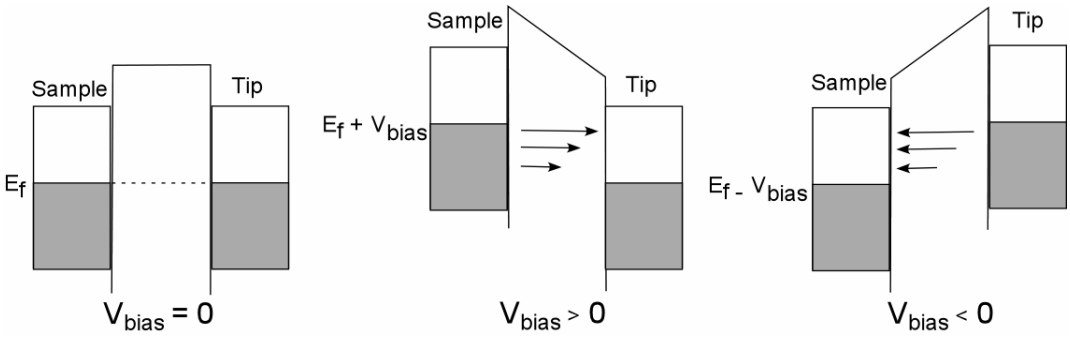

Figure 2: Schematic of a metal-insulator-metal tunneling junction. The grey area represents electron filled states (occupied level) and the white area is empty states, ready to accept electrons (unoccupied level).

STM images represent the local magnitude of the tunneling current in the x-y plane. As the tunneling current strongly depends on the tip-sample distance (i.e., the width of the vacuum gap or insulator air gap) the convoluted information it provides are composed of (a) topographical changes and (b) surface electronic anisotropy.

Tunnel Current, Vacuum Gap Size and Density of States

The tunneling current decays exponentially with the distance gap distance z, and is strongly affected by the density of states (DOS) of the sample at the Fermi level, $\rho_s(E_f)^2$; i.e.,

$$I \propto V_{bias}\rho_s(E_F)\exp\left[-2\frac{\sqrt{2m(\phi-E)}z}{\hbar}\right] \propto V_{bias}\rho_s(E_F)\exp(-1.025\sqrt{\phi}\cdot z), \quad (1)$$

where m is the mass of electron and $\hbar$ is the Planck's constant.

An electronic state describes a specific configuration, an electron can possess. For instance, it can have either a spin up or spin down, or a particular magnetic momentum etc. A state is described by a set of quantum mechanical numbers. Each state can only be filled by one electron. Consider a classroom of X chairs with Y < X students. The chairs represent the states and the students the electrons. Let us assume, it is hard to read the board, and the students are all very interested in the subject. Consequently the chairs will be filled up towards the front with some empty seats in the back. This situation is illustrated in Figure 3. The chairs in each row are represented by circles. Filled circles represent student occupied chairs. The distance from the board is indicated with x. The number of chairs per row represents the density of states (DOS) for a particular classroom. Two distinctly different classrooms are shown in Figure 3. In the second classroom N is a function of the x. The last row that is filled is identified by x_F. Returning to electrons in metals; x_F corresponds to the Fermi energy E_f, N to ρ_s and N(x_F) to $\rho_s(E_f)$. In the case of the free electron model for s-/p-metals at zero Kelvin, $\rho_s(E)$ is proportional to the square root of the energy.

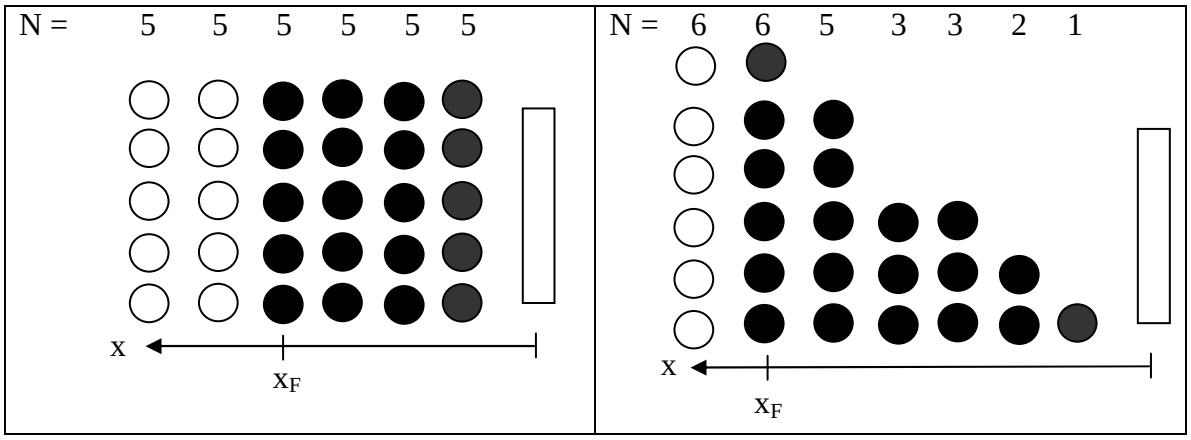

Figure 3: Density of state (DOS), N, and Fermi energy x_F in two classroom settings. (left) N is constant. (right) N(x).

Many physical properties are affected or depend on the number of states within an energy range (i.e., the energy density of states). While in metals and semi-metals, there is relatively small variation in the density of states due to the large electron delocalization, the density of energy levels in semiconductors varies noticeably. Thus, knowledge about DOS is of immense importance for electronic applications involving semiconducting materials, where the availability of empty valence and conduction states (states below and above the Fermi level) is crucial for the transition rates. In comparison to Figure 2 that visualizes tunneling between metals, Figure 4 illustrates the tunneling mechanism involving a semiconductor. The filled area (grey) is not uniform, representing the variation in electron density, and the lines in the unoccupied levels represent the variation in density of the energy levels that the tunneling electrons can occupy.

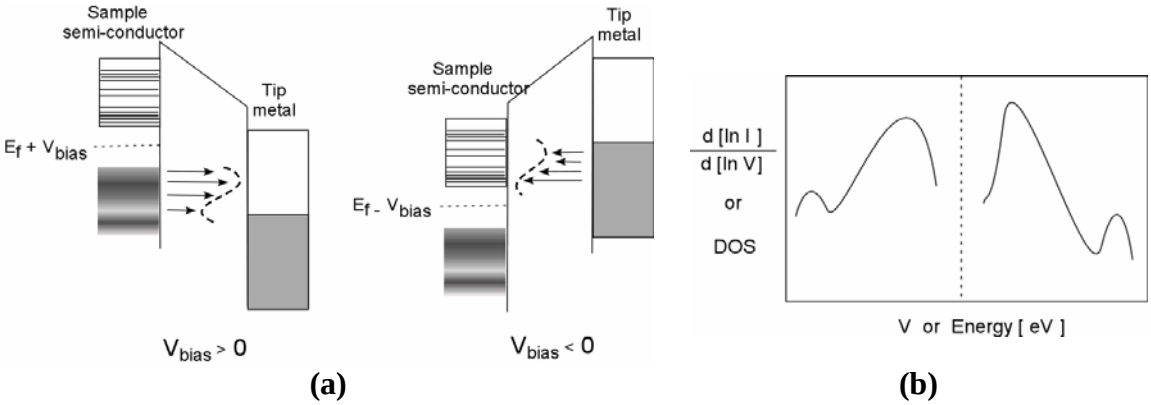

Figure 4: (a) Schematic of a metal-insulator-semiconductor tunneling junction and **(b)** corresponding normalized differential tunneling conductance.

STM and Local Density of States

STM constant current maps provide information about the variations in the electron density, and do not necessarily correspond to the location of atoms (nuclei). Figure 5 illustrates that a location of high tunneling current in a STM image can be either a compounded affected of two atoms, leading to a current maximum in between the atoms, or be identical with the location of an atom. This is for instance found for the silicon (001) 2x1 surface.[3] A π molecular orbital of the silicon-silicon dimers (Si=Si) creates the highest electron density (probability) at the center of the dimers, while an anti-bonding π^* molecular orbital has a node (a location where the probability is zero) at the center of the dimers. Thus, when a negative bias is applied, the electrons in the π-molecular orbital (occupied state) tunnel and the resulting image, similar to the case shown in Figure 5(a), will be obtained. When a positive bias is applied, the electrons of the tip tunnel into the anti-bonding π^* molecular orbital (unoccupied state), revealing a gap between the dimers, as in Figure 5(b). When the variation in the local DOS (LDOS) of metals is small, the contour of STM images often can be safely interpreted as the topography of the atomic lattice.[†]

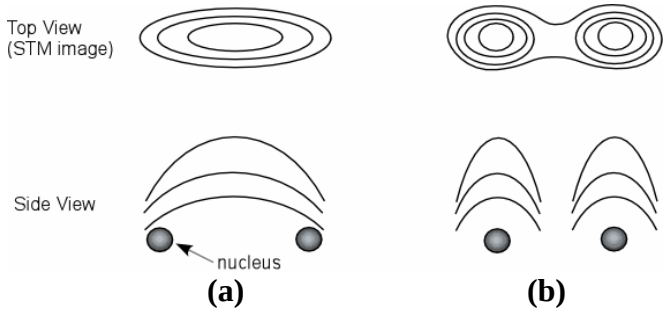

Figure 5: Sketch of possible STM images relative to the nucleus locations. Top view is the contouring lines of STM images and the corresponding side view on the bottom. STM image shows high tunneling location **(a)** at center of two nuclei and **(b)** at the top of each nucleus.

STM Measuring Modes

STM can be operated in three major operation modes: (1) imaging mode, (2) spectroscopy mode, and (3) manipulation mode. There are two imaging modes: Constant

[†] See next section on LDOS on variety of systems.

current imaging and constant height imaging. In constant current imaging, the vacuum or air insulating gap, *z*, between the tip and the sample is controlled by a current feedback control system. Scanning results in a constant current map of the surface. In contrast, the feedback is turned off, and the tip is scanned at a sample topography independent constant height, which results in a locally changing tunneling current map.

The spectroscopy STM mode, involves either a bias voltage V_{bias} sweep, or distance *z* ramping. The resulting current *I* is monitored as a function of the changing parameters. According to Equation (1), the tunneling current exhibits a log-linear gap distance z relationship. A simplified form of Equation (1) can be used to estimate the barrier height, ϕ, of the tunneling current, i.e.,

$$Log(I) = -A\sqrt{\phi} \cdot z + C \qquad (2)$$

where A is $1.025\sqrt{eV}$ /Å, and C is a constant. I-z spectroscopy is useful for the characterization of the quality of the STM tip, its sharpness and cleanliness. In the groundbreaking article of Binnig and Rohrer, the sensitivity of a STM tip was attained by the I-z curves and was observed to increase with successive cleaning procedures.

Tunneling spectroscopy as a function of the bias voltage, i.e., I-V curves, provides very important information about the surface electronic structure, such as the barrier heights and LDOS of the sample. While the experimental procedures is very similar for large variety of sample systems, i.e., the current is measured as a function of V_{bias}, the data analysis varies from system to system and is in more detail discussed below. As summarized in Figure 6, I-V spectroscopy offers with a first order analysis information about the electronics structure, and a second order analysis information vibrational mobilities.

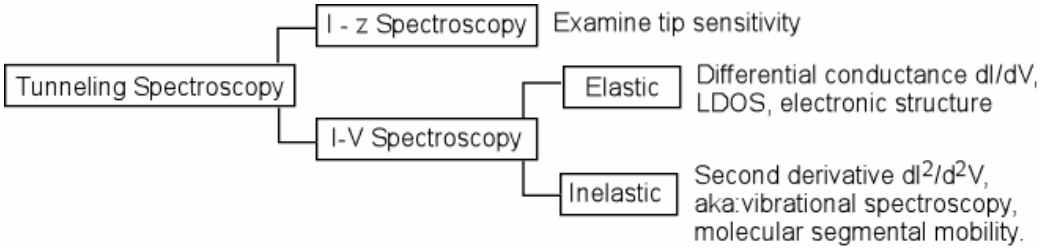

Figure 6: Modes of tunneling spectroscopy.

3. Tunneling Spectroscopy

In the STM imaging mode, the tunneling current *I* is continuously recorded at each location (*x*,*y*) at a constant bias voltage V_{bias}, generating a two-dimensional map of tunneling conductance I/V_{bias}. In contrast, tunneling spectroscopy (I-V curve) focuses on the tunneling conductance, or commonly, a normalized differential tunneling conductance $(dI/dV)/(I/V) = d[\ln(I)] / d[\ln(V)]$. Tunneling spectroscopy studies are usually performed without scanning at a particularly chosen location, based on an initial STM current or height map. However, it is also possible to scan while the bias is ramped (scanning tunneling spectroscopy (STS). Consider the aforementioned example, silicon 001 (2x1), it is evident that the spectroscopy at a location right above a nucleus would exhibit a I-V curve that is different from that of a center of two nuclei. In fact I-V spectroscopy on silicon 111 (7x7) surface is location specific.[4] Interestingly the average I-V curves at various locations closely resembles to data obtained by ultraviolet photoelectron spectroscopy (UPS) and inverse photoemission spectroscopy (IPS). It

suggests that UPS and IPS are the area average of the differential conductance, while STM tunneling spectroscopy is capable of resolving local information, e.g. local DOS rather than average DOS.

The general profile of the density of state around the Fermi level, i.e., $(\mathrm{d}I/\mathrm{d}V)/(I/V)$, can be used to classify the material based on its conductivity, as illustrated in Figure 7. As shown, metals do not possess a gap between the occupied states (valence band) and the unoccupied states (conduction band) and the variation in DOS is relatively small. Thus, the I-V curves are linear for the most part, resulting in a very small dI/dV gradient. Semi-metals also do not have a gap between the occupied and unoccupied states. There is, however, a gap in the momentum space (the waves are out of phase) that depresses the conductance around the Fermi level, and consequently bends the density of states at low voltages. For semiconductors and insulators, the conductance around the Fermi level is zero. The threshold voltage, i.e., band gap, $E_g = |V_{+bias}| + |V_{-bias}|$, is relatively small for semiconductor (< 3eV, used as definition for semiconductors). As shown in Figure 7, semiconductors show a highly bend DOS, which is flat as for insulators at low voltages, where the energy gap E_g cannot be bridged. It is well known that doping semiconductors with impurities or defect sites affect reduce E_g , and thus, can modify the density of states at the Fermi level to such a degree that it resembles nearly a semi-metal.

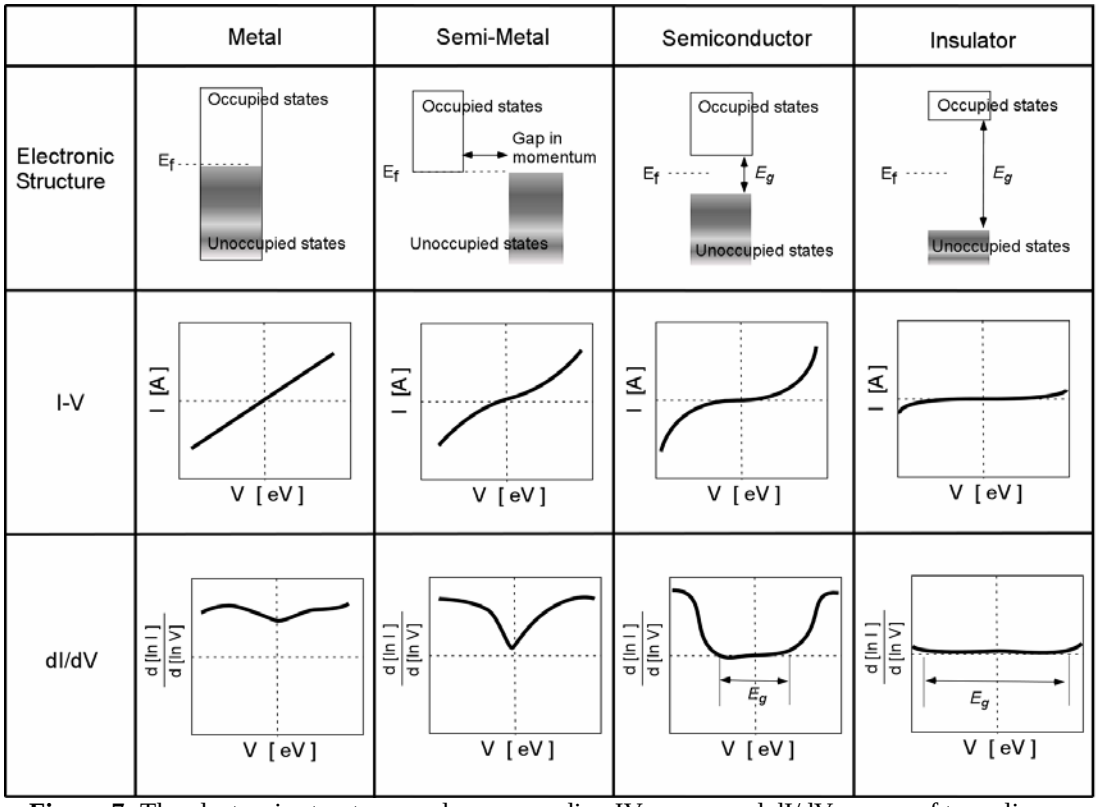

Figure 7: The electronic structures and corresponding IV curves and dI/dV curves of tunneling spectroscopy.

So far, we have discussed elastic tunneling spectroscopy, in which the energy of the tunneling electrons is conserved. In inelastic tunneling spectroscopy, the counter electrode is not the material under investigation; rather it is the gap that is examined. In

general, the material of interest is placed on top of the counter electrode or fills the insulating gap completely as a thin film. When the tunneling current travels through the material, a part of tunneling electron energy is dissipated by activating various modes of the molecular motion, e.g. C-H stretching of hydrocarbon chains. Thus the modes of the molecular motion can be deduced based on the extensive data base of infrared spectroscopy (IR). Experimentally, the I-V curve is obtained in the same manner as the elastic tunneling spectroscopy. To identify the modes of the molecular motion, the second derivative, dI^2/d^2V, is calculated, which contain multiple number of sharp peaks. The modes of molecular motion are then identified by the locations of the peak V_{peak}.

4. Layered Structure of HOPG

Highly ordered pyrolytic graphite (HOPG) consists of layers of carbon sheets, forming a semi-metallic system. While the carbons within a sheet are covalently bonded to form a hexagonal lattice structure, the layers are held together by Van der Walls forces. The in-plane lattice constant (repeating unit length) and the z-axis lattice constant are 2.46Å and 6.7 Å respectively and the in-plane atom-to-atom distance is 1.42 Å. The sheets are arranged such that the every other carbon on a layer has a carbon in the neighboring sheets, Figure 8. The carbons in the first layer that have a carbon in the second layer right below are called an A-site carbons, and the carbons without a carbon directly below are called B-site carbons.

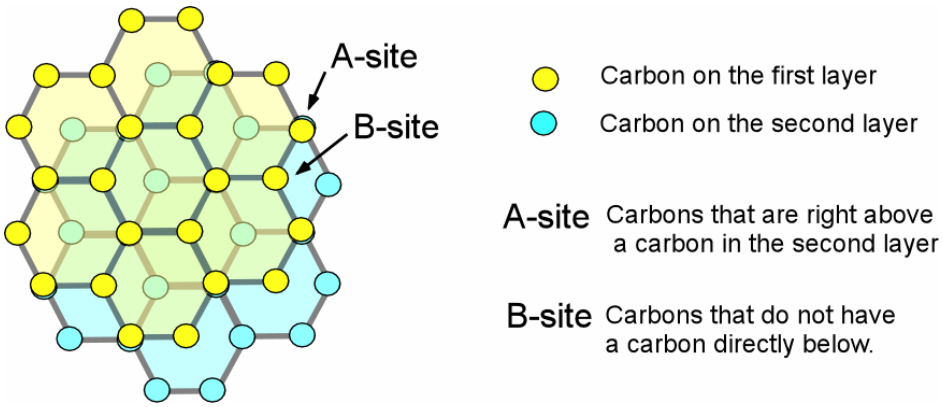

Figure 8: Layered structure of HOPG.

In STM images, the two types of carbons (A-site and B-site) appear differently. As shown in Figure 9, the B-site carbons exhibit a higher LDOS (i.e., topography) than the carbons at the A-site, exhibiting the *three-fold-hexagon* pattern.

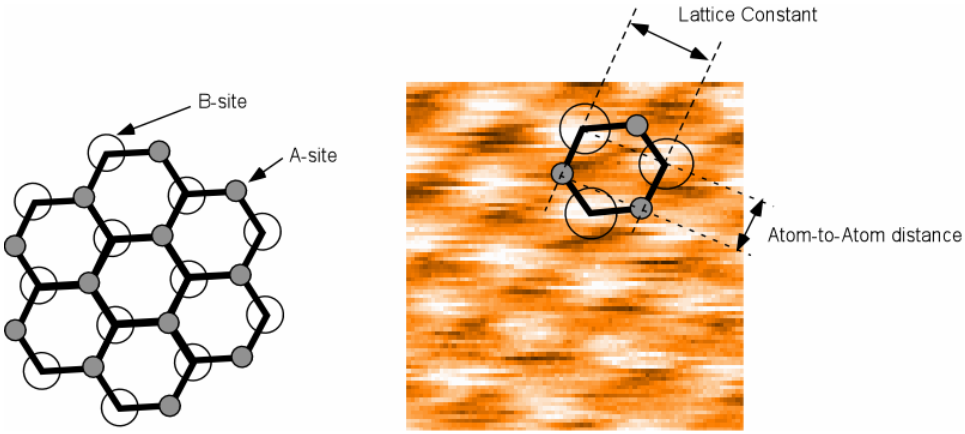

Figure 9: Interpretation of HOPG's *three-fold-hexagon* pattern of STM images

While most of STM study of HOPG shows this *three-fold-hexagon* pattern, there are reports on various other patterns of HOPG, such as true hexagon and linear row structure. A possible explanation is given by multiple tip artifacts. Simulations of multiple tip contacts showed superimposed signal collection.

References

1 G. Binnig, H. Rohrer, C. Berber, and E. Weibel, Appl. Phys. Lett. **40** (2), 178 (1981).

2 E. Meyer, H. J. Hug, and R. Bennewitz, *Scanning Probe Microscopy*. (Springer, Berlin, 2004).

3 R. J. Hamers and Y. J. Wang, Chemical Reviews **96** (4), 1261 (1996).

4 R. J. Hamers, R. M. Tromp, and J. E. Demuth, Phys. Rev. Let. 56 (18), 1972 (1986).

Recommended Reading

Quantum Chemistry and Spectroscopy by Thomas Engel and Philip Reid, Pearson/Benjamin Cummings, San Francisco, 2006.

Scanning Probe Microscopy and Spectroscopy, Methods and Applications, by Roland Wiesendanger, Cambridge University Press, Cambridge, 2rd ed. 1994.

Scanning Probe Microscopy-The lab on a Tip, by Ernst Meyer, Hans Josef Hug, Roland Bennewitz, Springer, Berlin, 2004.